Int. J. Solids Structures Vol. 28, No. 6, pp. 791–803, 1991
Printed in Great Britain.

0020–7683/91 $3.00 + .00

INFLUENCE OF RESIDUAL STRESSES ON HYDROGEN EMBRITTLEMENT SUSCEPTIBILITY OF PRESTRESSING STEELS

J. TORIBIO and M. ELICES
Department of Materials Science, Polytechnical University of Madrid, ETSI Caminos, Ciudad Universitaria, 28040 Madrid, Spain

(*Received* 18 *July* 1990; *in revised form* 14 *January* 1991)

Abstract—Hydrogen embrittlement is a general phenomenon which lowers the fracture resistance of high-strength steels, and therefore raises the failure risk of prestressing concrete structures. The Ammonium Thiocyanate Test (ATT) was proposed by the International Federation of Prestressing (FIP) as a suitable method for checking the hydrogen embrittlement susceptibility of prestressing steels. The main disadvantage of this test is the scattering of the results.

In this work a great number of experimental results at different applied stresses are analyzed in four pearlitic eutectoid steels. A diffusion model, based on both hydrogen concentration and hydrostatic stress gradients, is proposed. The residual stresses measured on the wire surface by X-ray diffraction are also considered in the model.

Times to rupture, as a function of applied stress, were obtained showing close agreement with the experimental data, and illustrating the role of previous residual stress distributions in hydrogen embrittlement, and so the increased scattering of the results when the externally-applied stress is lower.

1. INTRODUCTION

High-strength steel wires (ultimate tensile strength > 1500 MPa), usually cold-drawn eutectoid steels, are widely used for prestressing concrete structures. The importance of this steel may be reckoned from the world production, over 10^6 tonnes per year. Stress corrosion cracking (SCC) of prestressing steel is currently the subject of many studies (Parkins *et al.*, 1982), and there is general agreement that hydrogen embrittlement plays an important role in the environmental cracking of such a steel.

The International Federation for Prestressing (FIP) has proposed a test—the Ammonium Thiocyanate Test (ATT)—to determine the hydrogen embrittlement susceptibility of prestressing steels (FIP-78, 1981). In spite of some objections to this standard corrosion test method (Parkins *et al.*, 1981), it is still the best suited to steel control and acceptance. Thus, any contribution to a better understanding of the meaning of the ATT, and especially of the influence of stress levels on the time to rupture, should be welcome, both from the scientific point of view and for practical and economic reasons.

In this paper, the influence of internal residual stress distribution on the hydrogen embrittlement susceptibility of prestressing steels is analyzed through the Ammonium Thiocyanate Test. Residual stresses are introduced in the steel during the manufacturing process, so they can be considered as an intrinsic characteristic of the material, and represent a variable for the design of any steel structure.

The hydrogen transport model used in this study is based on hydrogen diffusion. Internal residual stresses in the material play an important role, since they transform a uniform stress state into a non-uniform one. The mathematical problem has no analytical solution, and it is here solved by numerical methods, discretizing the diffusion equations. The validity of the discretization was checked by solving a simpler problem with an analytical solution. Several residual stress distributions were introduced in the model, based on previous measurements on steels.

The final aim of this research is to obtain curves representing applied stress versus time to rupture of the high-strength steels, as a function of the different residual stress distributions in the wires. These curves allow a prediction of the life of the material in a hydrogen environment. Procedures such as surface rolling, useful in extending the life of the steel wires, are also proposed.

Table 1. Chemical composition

Steel	%C	%Mn	%Si	%P	%S	%N
A	0.82	0.60	0.18	0.010	0.024	0.007
B, C, D	0.81	0.60	0.27	0.014	0.029	0.011

Table 2. Mechanical properties

Steel	0.2% offset yield strength (MPa)	Ultimate tensile strength (MPa)	Elongation under U.T.S. (%)	Reduction of area (%)	K_{IC} (MPa m$^{1/2}$)
A	1455	1700	6.0	30.0	98
B	1460	1681	5.5	29.5	98
C	1410	1653	5.6	27.2	98
D	1460	1682	5.5	27.0	98

2. EXPERIMENTAL BASES

Four commercial prestressing steel wires were tested (Piñero, 1981; Sánchez-Gálvez and Elices, 1984). Their chemical compositions are shown in Table 1 and their mechanical properties are summarized in Table 2. All of them were eutectoid cold-drawn steels, produced by patenting 12 mm diameter rods in a molten lead bath at 530°C for about 10 s to produce fine pearlite, after which the rods were cold drawn to achieve 7 mm diameter wires. Finally, the drawn wires were stress-relieved at 425°C for a few seconds and cooled in water (steels A, B and D) or in oil (steel C).

The specimens used for testing were smooth round wires with their surface in the as-delivered condition. Samples were degreased with trichlorethylene and loaded at a constant load by means of levers. If no fracture occurred in a given time, the specimen was unloaded and the time recorded, in order to obtain a threshold stress value. This was never less than 600 hours. For each stress level, at least four tests were performed, and in many cases eight tests were carried out.

The results are shown in Fig. 1 for the four tested steels and the two test temperatures (35 and 50°C). For each stress level σ_{ap}, the average time to rupture t_R and the interval corresponding to the standard deviation are plotted. Two considerations must be made:

—These tests present a high level of scattering in time to rupture, a variable which reflects the susceptibility of the metal to hydrogen embrittlement.

—The scattering is non-uniform: for high stress levels it is small, and clearly increases when the applied stress is lower.

The explanation should be sought in any variable able to modify the externally-applied stress state. Internal residual stresses in the material have been proposed as the cause of these phenomena (Elices *et al.*, 1983; Campos and Elices, 1986).

3. THEORETICAL MODEL

3.1. *Diffusion*

The theoretical hydrogen diffusion model is based on two main hypotheses:

(D1) TRANSPORT: The main hydrogen transport mechanism is diffusion, therefore neglecting transport by movement of dislocations, according to the authors' previous research with this kind of steel (Toribio, 1987; Toribio and Elices, 1988, 1990), and other general studies on hydrogen embrittlement of steels with cathodic charging during the test (Hirth, 1980).

(D2) ABSORPTION: The absorption of adsorbed hydrogen at the surface is quasi-instantaneous, as is demonstrated in previous works by Toribio (1987) and Toribio and Elices (1988, 1990). In fact, even in very fast hydrogen embrittlement tests, the loss of

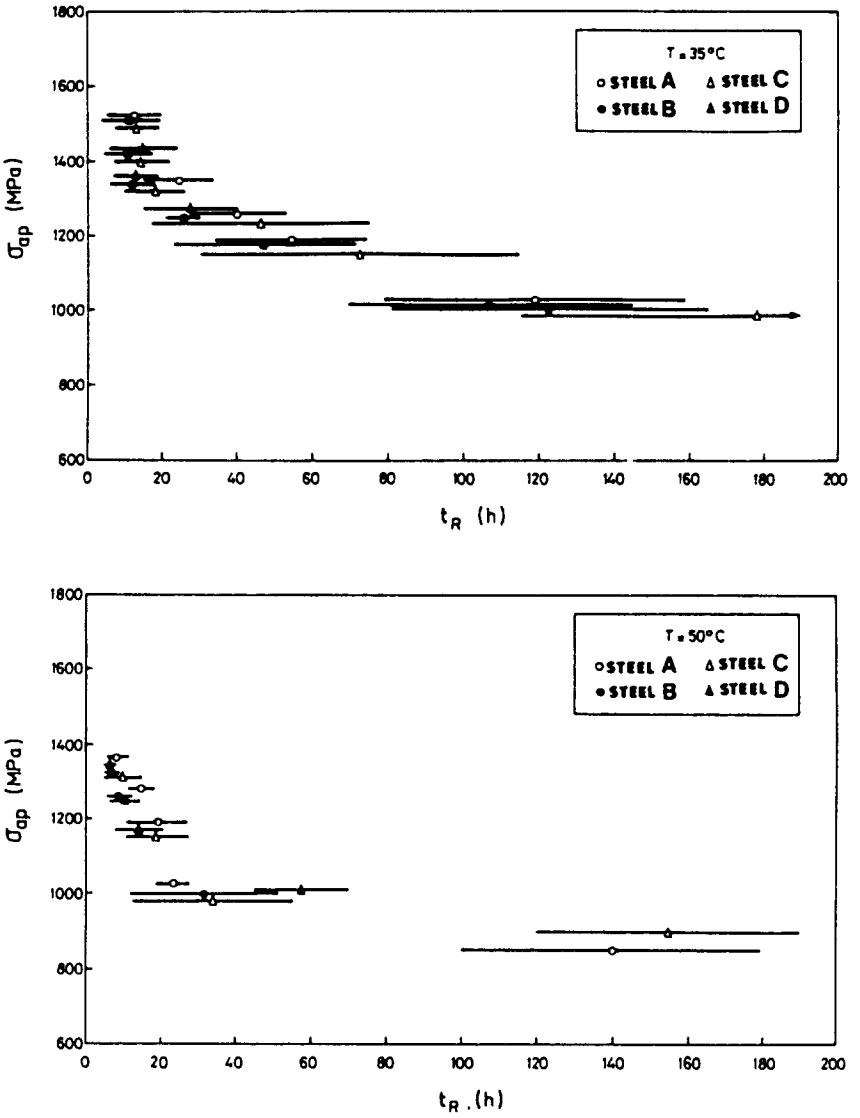

Fig. 1. Experimental results of the FIP test.

fracture load with respect to the air test is relevant. The damage produced by the hydrogen (embrittlement) is not negligible despite the shortness of the tests.

The strain rate required for the hydrogen embrittlement effect to be negligible is that of a test duration of around 10 s. The absorption time will be even shorter, which indicates a test duration negligible in comparison with the usual ones (10–200 hours).

The diffusion equations are Fick's Laws, modified to include terms dependent on the hydrostatic stress (Van Leeuwen, 1972, 1974, 1977; Astiz, 1984, 1987):

$$\mathbf{J} = -D\,\mathbf{grad}\,c + Mc\,\mathbf{grad}\,\sigma \tag{1}$$

$$\frac{\partial c}{\partial t} = D\,\Delta c - M\,\mathrm{grad}\,c \cdot \mathrm{grad}\,\sigma - Mc\,\Delta\sigma \tag{2}$$

where c is the hydrogen concentration, σ is the hydrostatic stress ($\sigma = \sigma_{ii}/3$), D the diffusion coefficient and M a second coefficient dependent on the latter:

$$M = \frac{DV^*}{RT} \tag{3}$$

and V^* is the molar partial volume of hydrogen, R the ideal gases constant and T the absolute temperature.

The concentration of absorbed hydrogen in the boundary is, according to D2:

$$c_0^* = c_0 \exp\left(\frac{V^*\sigma}{RT}\right), \tag{4}$$

Boltzmann's distribution where c_0 is the equilibrium concentration without stresses, and σ the hydrostatic stress at the boundary.

The problem to solve (Fig. 2) is the one referring to a cylinder of radius a and $c = c_0^*$ as the value of hydrogen concentration at the boundary ($r = a$, adopting r and z as the cylindrical coordinates). Taking into account the cylindrical symmetry, the diffusion equation leads to:

$$\frac{\partial c}{\partial t} = D\left(\frac{\partial^2 c}{\partial r^2} + \frac{1}{r}\frac{\partial c}{\partial r}\right) - \frac{DV^*}{RT}\frac{\partial c}{\partial r}\frac{\partial \sigma}{\partial r} - \frac{DV^*}{RT}c\left(\frac{\partial^2 \sigma}{\partial r^2} + \frac{1}{r}\frac{\partial \sigma}{\partial r}\right) \tag{5}$$

in the interval $0 \leqslant r \leqslant a$, with the initial condition:

$$c(r, 0) = 0; \quad 0 \leqslant r \leqslant a \tag{6}$$

and the boundary conditions:

$$\frac{\partial c}{\partial r}(0, t) = 0; \quad t \geqslant 0 \tag{7}$$

$$c(a, t) = c_0^*; \quad t \geqslant 0. \tag{8}$$

The boundary condition (7) is due to the symmetry of the problem: the hydrogen flux just at the cylinder axis ($r = 0$) is zero. Condition (8) yields $c = c_0$ when the solid is free of stress.

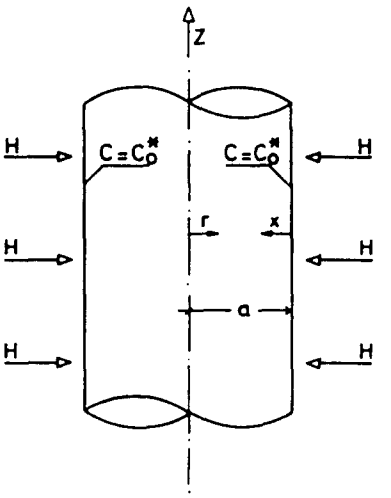

Fig. 2. Problem to solve.

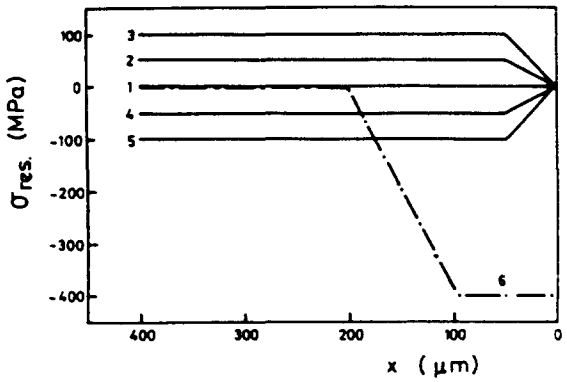

Fig. 3. Residual stress distributions.

In this research the influence of the axial residual stress distribution in the cylinder is analyzed. To achieve this, six kinds of distribution are considered (see Fig. 3, where x is the depth from the boundary of the cylinder). Since the critical crack depth is never greater than 350 μm, only 400 μm of residual stress distributions have been plotted. Outside this region, the equilibrium conditions are applied. Distribution 1 corresponds to the material without stresses. Distributions 2, 3, 4 and 5 are typical distributions measured in commercial wires by Campos and Elices (1986). Distribution 6 models a rolling process on the wire, and allows a study of the benefits of such a technique, increasing the time to rupture.

Equation (5) with conditions (6), (7) and (8) has no analytical solution, and so the Finite Element method for the stress–strain problem was used together with a Weighted Residuals formulation for the diffusion problem (Astiz, 1984, 1987). The domain was discretized according to the mesh shown in Fig. 4, more refined in the area next to the boundary of the sample, to reproduce adequately the residual stress distributions of Fig. 3. The program gives the hydrogen concentration at the mesh nodes. The residual stresses were introduced as initial values at the integration (Gauss) points. The discretization time interval was $D\Delta t/a^2 = 0.01$, cf. Astiz (1987).

The space discretization was checked by solving a specific problem with an analytical solution: the diffusion in a cylinder free of stress. In this case, eqn (5) becomes:

$$\frac{\partial c}{\partial t} = D\left(\frac{\partial^2 c}{\partial r^2} + \frac{1}{r}\frac{\partial c}{\partial r}\right) \tag{9}$$

in the interval $0 \leqslant r \leqslant a$, with the initial condition (6) and the boundary conditions (7) and (8), the latter with value c_0 as a particular case.

The solution is (Kikuta *et al.*, 1972; Crank, 1975; Budak *et al.*, 1984):

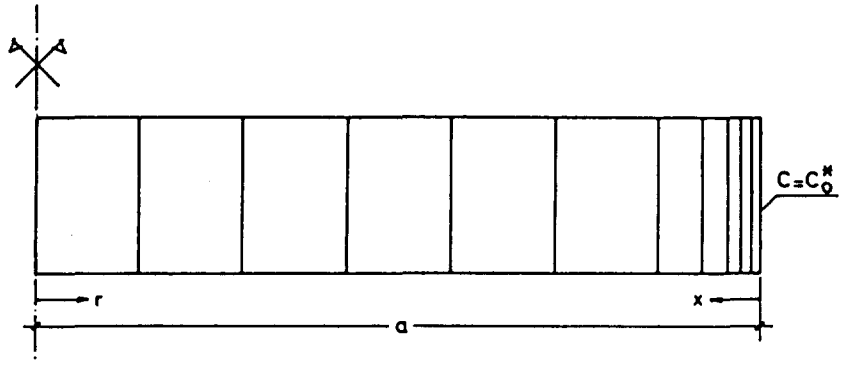

Fig. 4. Discretization of the domain.

$$\frac{c}{c_0} = 1 - \frac{2}{a} \sum_{n=1}^{\infty} \frac{J_0(\alpha_n r)}{\alpha_n J_1(\alpha_n a)} \exp(-D\alpha_n^2 t) \tag{10}$$

where J_0 and J_1 are the Bessel functions with orders zero and one, respectively, and α_n the positive roots of the equation $J_0(\alpha_n a) = 0$. The first 10 roots of this equation are:

$x_1 = 2.4048.$ $x_2 = 5.5201.$ $x_3 = 8.6537.$ $x_4 = 11.7915.$ $x_5 = 14.9309.$

$x_6 = 18.0711.$ $x_7 = 21.2116.$ $x_8 = 24.3525.$ $x_9 = 27.4935.$ $x_{10} = 30.6346.$

The Bessel functions can be extended in series:

$$J_n(x) = \sum_{k=0}^{\infty} \frac{(-1)^k (x/2)^{n+2k}}{k!\Gamma(n+k+1)} \tag{11}$$

where Γ is the Euler gamma function, which for an integer variable, as in the case of this problem, has the following expression:

$$\Gamma(p) = (p-1)! \tag{12}$$

The analytical solution (exact) is compared in Fig. 5 with the numerical one. The agreement is excellent for the time interval adopted ($D\Delta t/a^2 = 0.01$), and the maximum errors are never above 4%. This interval, therefore, will be used in the diffusion computations in all samples.

3.2. *Fracture*

The following hypotheses are adopted regarding fracture:

(F1) INITIATION: Fracture initiates when the hydrogen reaches a critical concentration c_c over a distance x_c (damaged zone or critical size for initiation); then it is assumed that a crack with depth x_c is created.

(F2) PROPAGATION: The propagation time, i.e. the time required to propagate the crack from the initial size x_c up to a critical value to produce the final rupture of the sample, will be neglected. That is, it is assumed that the initiation time coincides with the time to rupture. Such an assumption was proved experimentally by Piñero (1981), by measuring the compliance of the sample, which remained constant during the test, even for the steps just before the final fracture. Furthermore, Piñero (1981) proved also that, on testing in tension degasified samples unloaded after 90% of the expected time to rupture, no changes in the tensile strength were observed.

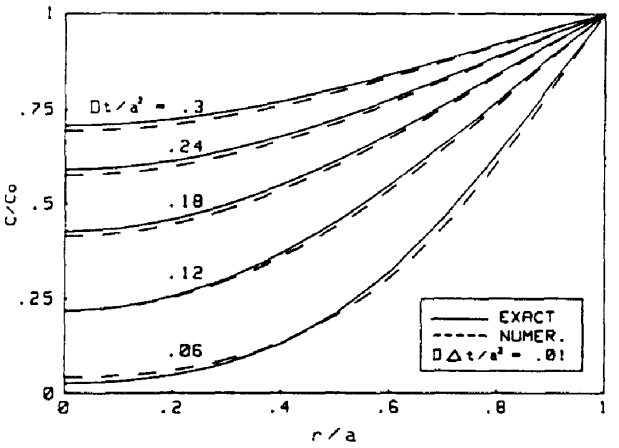

Fig. 5. Exact and numerical solutions for the diffusion in a cylinder free of stress.

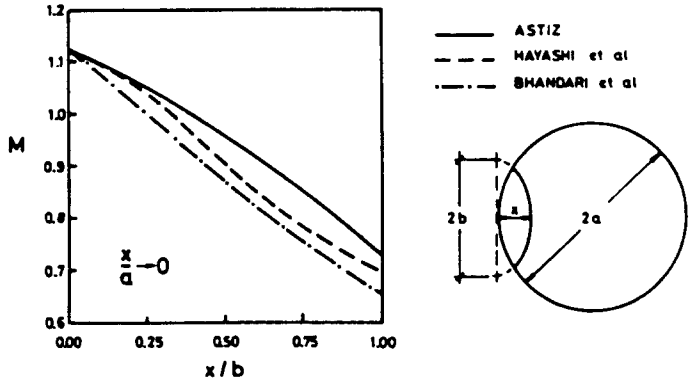

Fig. 6. Stress intensity factor for a semi-elliptical crack in a cylinder [from Elices (1985) and Astiz (1986)].

With both hypotheses the solution of the problems requires the knowledge of the time to rupture t_R, at which the hydrogen reaches a critical concentration c_c over a critical distance x_c. The fracture condition is based on the stress intensity factor:

$$K_I = K_{IHE} \tag{13}$$

where K_{IHE} is the threshold stress intensity factor for the hydrogen environment.

The expression for the stress intensity factor is, for this problem,

$$K_I = M(\sigma_{ap} + \sigma_{res})\sqrt{\pi x} \tag{14}$$

in which M is a non-dimensional factor dependent on the geometry, σ_{ap} the applied stress and σ_{res} the residual stress prior to cracking. Equation (14) is only valid for uniform residual stress distribution, and those considered in Fig. 3 are not constant. However, they are considered uniform in order to calculate the stress intensity factor (the error is negligible), but not to study the diffusion.

The value M was calculated by Elices (1985) and Astiz (1986) for uniform tension loading. Figure 6 shows a plot of the dimensionless factor M versus the crack aspect ratio x/b for the shortest cracks ($x/a \to 0$), which is the case of the zone damaged by the hydrogen, never above 400 μm (a = 3.5 mm, since the wire diameter is 7 mm). A value $M = 0.94$ was adopted, which corresponds to a relation $x/b = 0.5$. The fracture condition is, thus:

$$0.94(\sigma_{ap} + \sigma_{res})\sqrt{\pi x_c} = K_{IHE}. \tag{15}$$

4. LIFE PREDICTION

The final aim of this research is to determine the time to rupture of these steels in hydrogen environment. To achieve this, it is necessary to calculate the evolution of the hydrogen concentration at each point of the sample. The computational program provides, at each step of loading, the nodal concentrations. By using an interpolation both in space and time, it is possible to discover the hydrogen concentration at all points and instants. Fracture will take place in an instant t_R at which the critical hydrogen concentration c_c is reached over a critical distance x_c.

The following computation data were adopted:

- $V^* = 2\ \text{cm}^3\ \text{M}^{-1}$, according to Hirth (1980).
- $D = 4.99 \times 10^{-12}\ \text{m}^2\ \text{s}^{-1}$ (35°C), $D = 10^{-11}\ \text{m}^2\ \text{s}^{-1}$ (50°C), taken from the papers by Elices *et al.* (1980) and Doig and Jones (1977). An activation energy for hydrogen diffusion of 9000 cal M^{-1} was assumed (Piñero, 1981).
- $c_c/c_0 = 1.24$ (35°C), $c_c/c_0 = 1.18$ (50°C), taken from Sánchez-Gálvez and Elices (1984).

- $K_{IHE} = 0.27\ K_{IC}$, as was previously shown for all commercial prestressing steels in the ATT solution (Elices *et al.*, 1981).

The results of the diffusion computation for the most representative residual stress distributions (3, 5 and 6) are shown in Fig. 7, which offer the hydrogen concentration at each point of the sample at any time. It can be easily observed how the residual stress gradients affect the hydrogen diffusion.

Tensile stresses (distribution 3) enhance the hydrogen flux towards the inside; compressive stresses (distribution 5) delay it. Distribution 6, corresponding to a surface rolling, presents a minimum concentration at the maximum hydrostatic compression point, and ahead an increment due to the strong tension gradient. It must be borne in mind in this case that the boundary concentration c_0^*, given by eqn (4), is very small because of the high compressive residual stress at the boundary.

To obtain the curves for applied stress σ_{ap} versus time to rupture t_R and compare them with the experimental results given in Fig. 1, the procedure is as follows: for each applied stress, the critical zone is calculated by means of:

$$x_c = \frac{1}{\pi}\left[\frac{K_{IHE}}{0.94(\sigma_{ap}+\sigma_{res})}\right]^2 \tag{16}$$

derived from (15), in which σ_{res} represents the residual stress value for the horizontal part of the curves given in Fig. 3.

On the other hand, the non-dimensional critical concentration is, with respect to the boundary concentration:

$$\frac{c_c}{c_0^*} = \frac{c_c/c_0}{\exp\left[(\sigma_{ap}+\sigma_{res,c})V^*/RT\right]} \tag{17}$$

where $\sigma_{res,c}$ is the residual stress at the boundary ($r = a$), with value zero in all residual stress distributions except number 6.

The critical depth (16) and the critical concentration (17) are introduced in the diffusion results (concentration in all points of the sample for any time, Fig. 7). First of all, the hydrogen concentration in the x_c depth point in any instant is calculated (from the nodal concentrations); later, the time for which such a concentration reaches the value c_c/c_0^* is obtained.

Figure 8 shows the results from the theoretical model (one line for each residual stress distribution) compared with the experimental results (shaded area). The agreement is excellent, because curve 1—which corresponds to a material without residual stresses—exactly fits the central tendency, and curves 2, 3, 4 and 5—which correspond to materials with residual stresses associated with the manufacturing process—cover the experimental band with very good agreement. Compressive residual stresses extend the lifetime of the wires, and tensile residual stresses decrease it. Curve 6 corresponds to a material which has suffered a rolling process after manufacture, introducing strong compressive residual stresses which clearly extend the life, as has been previously observed by Campos and Elices (1986).

The importance of the externally-applied stress in the scattering of the results (higher for lower stresses) is pointed out, since for lower externally-applied stress the role of internal residual stresses is more important.

The different results at both temperatures can also be observed, given the dependence of the diffusion coefficient on this variable. It is very important, therefore, to control as accurately as possible the temperature during the Ammonium Thiocyanate Test, since small variations in the temperature can produce strong variations in the time to rupture.

Finally, the stress-free solutions for the hydrogen diffusion in a cylinder (as used in this paper) and in a half-plane (approximate problem widely used because of its analytical solution) are compared. The solution for the half-plane is:

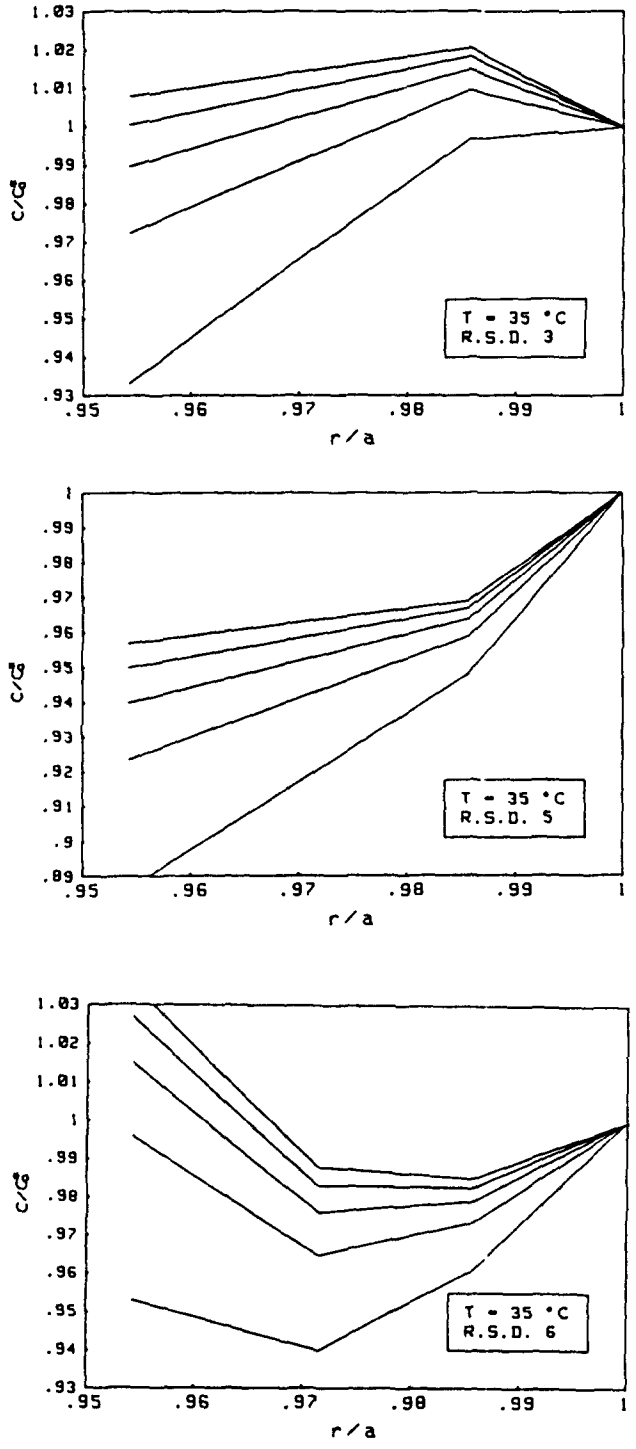

Fig. 7. Results of the diffusion computations for the different residual stress distributions (RSD).

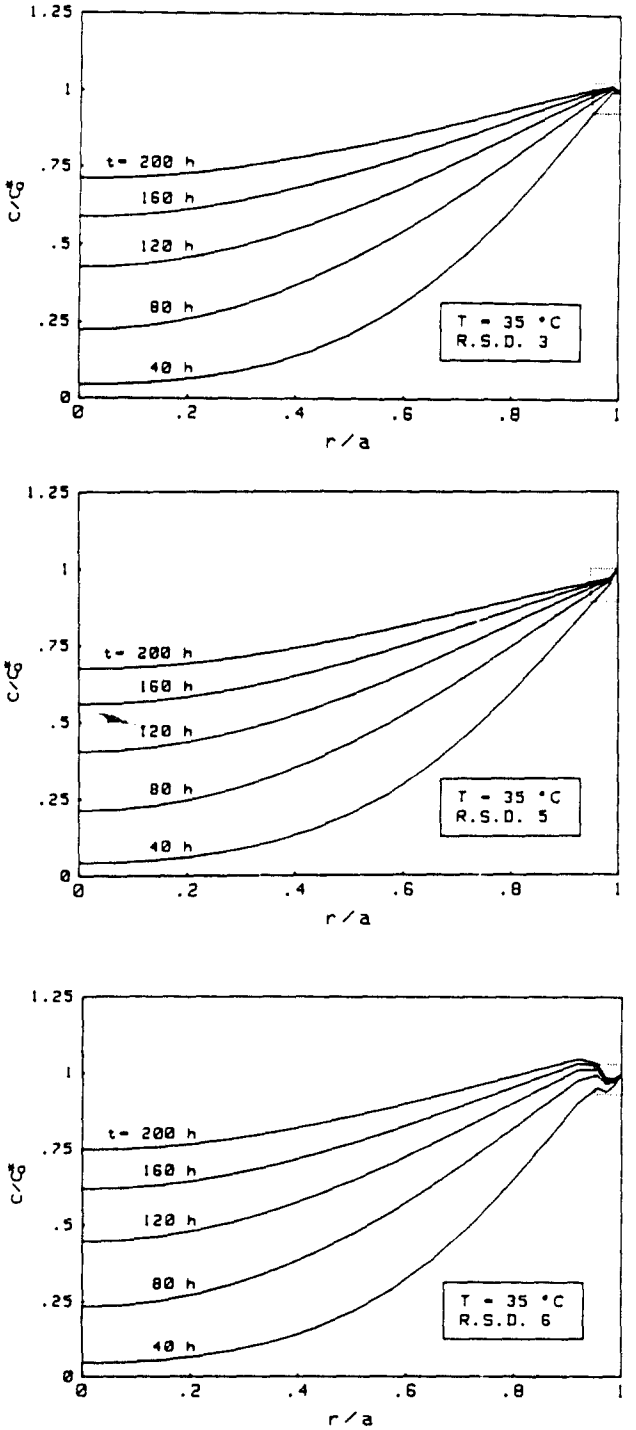

Fig. 7. (*Continued*).

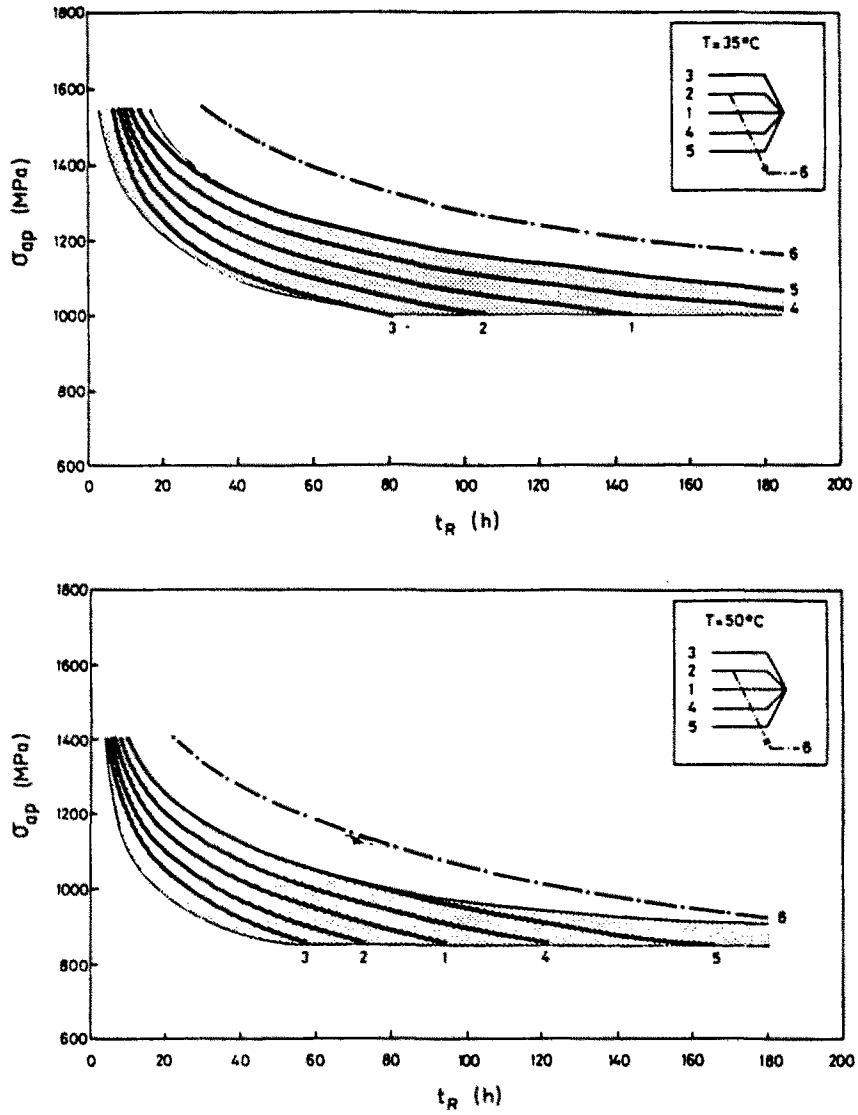

Fig. 8. Comparison between theoretical model and experimental results (shaded area).

$$\frac{c}{c_0} = 1 - \operatorname{erf}\left[\frac{x}{2(Dt)^{1/2}}\right] \tag{18}$$

where the error function is:

$$\operatorname{erf} z = \frac{2}{\sqrt{\pi}} \int_0^z \exp(-y^2)\, dy. \tag{19}$$

In Fig. 9 the solutions for the cylinder are compared with those for the half-plane and also with the experimental scattering band. The approximate solution (half-plane) has an important error, and is non-conservative, since the predicted times to rupture are higher than the real values. The error increases when the applied stress is lowered, and for the lowest stresses the half-plane solution goes out of the experimental band.

5. CONCLUSIONS

(1) The influence of residual stresses on hydrogen embrittlement susceptibility of prestressing steels was theoretically modelled, obtaining a very accurate prediction of the experimental results, and covering the scattering band.

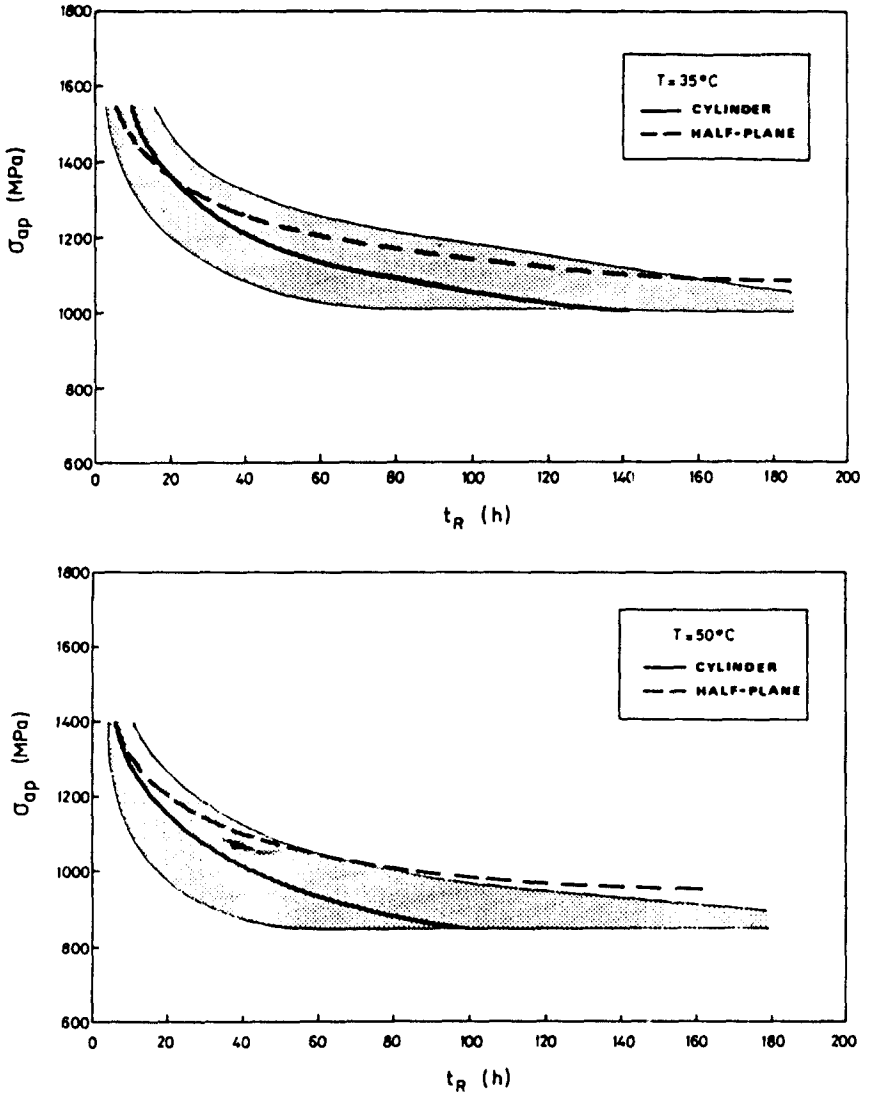

Fig. 9. Comparison between theoretical solutions for the cylinder and the half-plane (experimental results shown by the shaded area).

(2) The role of diffusion in the hydrogen transport in metals was confirmed, because the numerical model is able to explain the great differences in time to rupture among the different tests.

(3) The importance of the externally-applied stress in the scattering of the results (higher for lower stresses) is pointed out, since for lower externally-applied stresses the role of internal residual stresses is more important.

(4) The temperature of the test must be carefully controlled, because the diffusion coefficient is temperature-dependent. Results from tests performed at different temperatures are not directly comparable.

(5) Rolling processes clearly extend the life of the wires by introducing high compressive residual stresses, which delay the diffusion of hydrogen towards the inner areas.

REFERENCES

Astiz, M. A. (1984). Numerical modelling of hydrogen diffusion in metals. *Proc. 2nd International Conf. on Numerical Methods for Nonlinear Problems* (Edited by E. Oñate *et al.*), Barcelona, Spain.

Astiz, M. A. (1986). An incompatible singular elastic element for two and three dimensional crack problems. *Int. J. Frac.* 31, 105–124.

Astiz, M. A. (1987). Hydrogen diffusion analysis in metals. In *Computational Methods for Non Linear Problems* (Edited by C. Taylor *et al.*), pp. 271–299. Pineridge Press, Swansea.

Budak, B. M., Samarski, A. A. and Tijonov, A. N. (1984). *Problems on the Mathematical Physics*. Mir Publishers, Moscow.

Campos, J. M. and Elices, M. (1986). Influencia de las tensiones residuales en la fragilización por hidrógeno de alambres trefilados. *Anales Mecánica Fractura* **3**, 251–256.

Crank, J. (1975). *The Mathematics of Diffusion*. Oxford University Press, Oxford.

Doig, P. and Jones, G. T. (1977). A model for the initiation of hydrogen embrittlement cracking at notches in gaseous hydrogen environments. *Met. Trans.* **8A**, 1993–1998.

Elices, M. (1985). Fracture of steels for reinforcing and prestressing concrete. In *Fracture Mechanics of Concrete*. (Edited by G. C. Sih), pp. 226–271. Martinus Nijhoff, Dordrecht.

Elices, M., Maeder, G. and Sánchez-Gálvez, V. (1983). Effect of surface residual stress on hydrogen embrittlement of prestressing steels. *Br. Corros. Jnl.* **18**, 80–81.

Elices, M., Sánchez-Gálvez, V., Bernstein, I. M., Thompson, A. W. and Piñero, J. M. (1980). Hydrogen embrittlement of prestressing steels. In *Hydrogen Effects in Metals*. (Edited by A. W. Thompson and I. M. Bernstein), pp. 971–978. AIME, New York.

Elices, M., Sánchez-Gálvez, V. and Entrena, A. (1981) Stress corrosion testing of cold drawn steel wires in NH_4SCN solutions. K_{ISCC} measurements. *Proc. 3rd FIP Symp.* FIP-Berkeley, Wexham Springs, Slough, U.K.

FIP-78 (1981). Stress corrosion test. Technical Report No. 5, FIP, Wexham Springs, Slough, U.K.

Hirth, J. P. (1980). Effects of hydrogen on the properties of iron and steel. *Met. Trans.* **11A**, 861–890.

Kikuta, Y. Ochiai, S. and Araki, T. (1972). The diffusivity of hydrogen and its effect on the embrittlement of steel. *Proc. 1st. International Conf. on Hydrogen in Metals*. (Edited by P. Azou), Paris, France, pp. 293–299.

Parkins, R. N., Elices, M. and Sánchez-Gálvez, V. (1981). Some comments on the standardization of tests methods for prestressing steel. *Proc. 3rd FIP Symp.*, FIP-Berkeley, Wexham Springs, Slough, U.K.

Parkins, R. N., Elices, M., Sánchez-Gálvez, V. and Caballero, L. (1982). Environment sensitive cracking of prestressing steels. *Corr. Sci.* **22**, 379–405.

Piñero, J. M. (1981). Tenacidad de fractura de alambres frente a la fragilización por hidrógeno. Ph.D. Thesis, Polytechnical University of Madrid.

Sánchez-Gálvez, V. and Elices, M. (1984). On hydrogen induced cracking in prestressing steel wires. *Proc. 5th European Conf. On Fracture—ECF5—*. (Edited by L. Faña), Lisbon, Portugal, pp. 1003–1014.

Toribio, J. (1987). Fractura elastoplástica de alambres entallados. Ph.D. Thesis, Polytechnical University of Madrid.

Toribio, J. and Elices, M. (1988). Slow strain-rate technique applied to round-notched wires. *Corrosion 88—(NACE Corrosion Research Symposium*. (Edited by R. N. Parkins and F. P. Ford), St Louis, U.S.A., pp. 88–92.

Toribio, J. and Elices, M. (1990). Role of diffusion in the hydrogen transport in metals. *Proc. 8th European Conf. on Fracture—ECF8—*. (Edited by D. Firrao), Torino, Italy, pp. 451–460.

Van Leeuwen, H. P. (1972). Hydrogen Embrittlement of the Circumferentially Notched Round Specimen. Technical Report NLR TR72113U, Amsterdam, The Netherlands.

Van Leeuwen, H. P. (1974). The kinetics of hydrogen embrittlement: a quantitative diffusion model. *Engng Frac. Mech.* **6**, 141–161.

Van Leeuwen, H. P. (1977). A failure criterion for internal hydrogen embrittlement. *Engng Frac. Mech.* **9**, 291–296.